Heliyon 10 (2024) e31058

Contents lists available at ScienceDirect

Heliyon

journal homepage: www.cell.com/heliyon

Research article

A combination of chitosan nanoparticles loaded with celecoxib and kartogenin has anti-inflammatory and chondroprotective effects: Results from an *in vitro* model of osteoarthritis

Zahra Nabizadeh [a,b,c], Mahmoud Nasrollahzadeh [d,e], Benjamin Kruppke [e], Davood Nasrabadi [a,b,*]

[a] Nervous System Stem Cells Research Center, Semnan University of Medical Sciences, Semnan, Iran
[b] Department of Medical Biotechnology, Faculty of Medicine, Semnan University of Medical Sciences, Semnan, Iran
[c] Cellular and Molecular Research Center, Qom University of Medical Sciences, Qom, Iran
[d] Department of Chemistry, Faculty of Science, University of Qom, Qom, 37185-359, Iran
[e] Max Bergmann Center of Biomaterials, Institute of Materials Science, Technische Universität Dresden, 01069, Dresden, Germany

ARTICLE INFO

Keywords:
Drug delivery
Kartogenin
Osteoarthritis
Chitosan nanoparticles
Celecoxib

ABSTRACT

Loading drugs in drug delivery systems can increase their retention time and control their release within the knee cavity. Hence, we aimed to improve the therapeutic efficacy of celecoxib and kartogenin (KGN) through their loading in chitosan nanoparticles (CS NPs). Celecoxib-loaded nanoparticles (CNPs) and KGN-loaded nanoparticles (K-CS NPs) were prepared using the absorption method and covalent attachment, respectively, through an ionic gelation process. The morphology, particle size, zeta potential, polydispersity index (PDI), conjugation efficiency (CE), encapsulation efficiency (EE), the *in vitro* release of the drug from NPs, as well as MTT and hemolysis assays, were evaluated. Then, the IL-1β-stimulated chondrocytes were treated with CNPs and K-CS NPs, individually or in combination, to explore their potential chondroprotective and anti-inflammatory effects. CNPs and K-CS NPs showed sizes of 352.6 ± 22.5 and 232.7 ± 4.5 nm, respectively, suitable for intra-articular (IA) injection. Based on the hemolysis results, both NPs exhibited good hemocompatibility within the studied range. Results showed that treating IL-1β-pretreated chondrocytes with CNPs or K-CS NPs remarkably limited the negative effects of IL-1β, especially when both types of NPs were used together. Therefore, injecting these two NPs into the knee cavity may improve drug bioavailability, rapidly suppress inflammation and pain, and promote cartilage regeneration. Meanwhile, for the first time, the study investigated the effect of the simultaneous use of celecoxib and KGN to treat osteoarthritis (OA).

1. Introduction

Osteoarthritis (OA) is a disabling degenerative disease in which joint inflammation has a critical share in its onset and progression [1]. The presence of inflammatory cytokines such as tumor necrosis factor-α (TNF-α) and interleukin-1β (IL-1β) in the OA joint, along with cartilage features like avascularity, slow down the regeneration rate [2]. Although there are different therapeutic strategies for OA, none of them can fully restore normal joint function or reverse the disease progression because of the active inflammatory

* Corresponding author. Nervous System Stem Cells Research Center, Semnan University of Medical Sciences, Semnan, Iran.
E-mail addresses: davood.bn@gmail.com, davood.bn@semums.ac.ir (D. Nasrabadi).

https://doi.org/10.1016/j.heliyon.2024.e31058
Received 30 January 2024; Received in revised form 8 May 2024; Accepted 9 May 2024
Available online 10 May 2024

environment [3]. One of the most common treatments is drug therapy, which focuses on relieving the symptoms associated with OA [4]. Oral administration of non-steroidal anti-inflammatory drugs has disadvantages such as low drug concentration in knee joints and gastrointestinal side effects [5]. Hence, the intra-articular (IA) injection has attracted much attention due to several advantages, such as its ability to improve drug bioavailability, localize the drugs at the target site, relieve pain rapidly, and avoid systemic side effects [6].

Celecoxib, a nonsteroidal anti-inflammatory drug (NSAID), is a selective COX-2 inhibitor with poor aqueous solubility. It is commonly used for the treatment of rheumatoid arthritis, OA, and pain management [7]. Although IA injection of celecoxib is a practical approach to alleviate symptoms and prevent disease progression, the drug does not significantly promote cartilage regeneration in the damaged areas [8]. Therefore, the simultaneous use of an anti-inflammatory drug with an agent that induces cartilage regeneration is crucial to obtaining acceptable long-term results in OA treatment [8].

KGN, a small non-protein compound, promotes the proliferation, migration, and differentiation of chondrocytes and endogenous mesenchymal stem cells (MSCs) [9]. Therefore, it has both protective and regenerative effects on cartilage. KGN binds to filamin A (FLNA) and disrupts its interaction with core binding factor β (CBFβ) [9,10]. In the nucleus, CBFβ binds to a DNA-binding transcription factor (RUNX1), and this complex upregulates chondrocyte gene expression, leading to the increased synthesis of hyaline cartilage markers such as collagen-II and aggrecan [10]. Although direct injection of the drug into the knee joint offers more advantages than oral administration, the rapid clearance of the drug from the joint limits its advantages [5,11]. Therefore, many studies have combined drugs with different materials to enhance their retention time and regulate drug release in the knee cavity [6,12–14].

Chitosan (CS), a polymeric material obtained from the *N*-deacetylation of chitin, is utilized in various industries, such as cosmetics, food, pharmaceuticals, agriculture, and medicine due to its valuable biological properties [15,16]. These properties include a polycationic structure (-NH_3^+ sites), biocompatibility, non-toxicity, and biodegradability [15]. CS is also widely used in drug delivery systems because it can be covalently coupled to the carboxyl groups of pharmaceutical agents through its amino groups [6].

This study used the ionic gelation method [17], a simple and mild technique, to prepare NPs. Considering that inflammation hinders the effective treatment of OA [3], celecoxib was physically loaded onto the surface of formed NPs to enable faster release. Also, considering that conjugating hydrophobic drugs to CS can improve their aqueous solubility and biocompatibility [6,18,19], KGN was covalently linked to the CS polymer (K-CS) to enhance its solubility and regulate its release. Finally, the potential chondroprotective and anti-inflammatory effects of K-CS NPs and CNPs were investigated, individually or in combination, in an *in vitro* model of OA. This study aimed to enhance drug solubility, prolong their retention time in the joint cavity, and merge the anti-inflammatory characteristics of celecoxib with the chondroprotective and regenerative effects of KGN for OA treatment. Meanwhile, for the first time, the study investigated the combined effect of celecoxib and KGN on OA chondrocytes to treat OA.

2. Materials and methods

2.1. Materials

Tripolyphosphate (TPP), KGN, CS (75–85% deacetylation degree, Mw 50–190 kDa), acetic acid, *N*-(3-dimethylaminopropyl)-*N*'-ethylcarbodiimide hydrochloride (EDC) and *N*-hydroxysuccinimide (NHS), dialysis tube (MWCO 12000–14000 Da), Thiazolyl Blue Tetrazolium Bromide (MTT) and recombinant human IL-1β were purchased from Sigma–Aldrich Inc. (St. Louis, MO, USA). Celecoxib was a gift from Arasto Pharmaceutical Chemicals Inc. (Tehran, Iran). The human chondrocyte cell line (C28/I2) was obtained from the

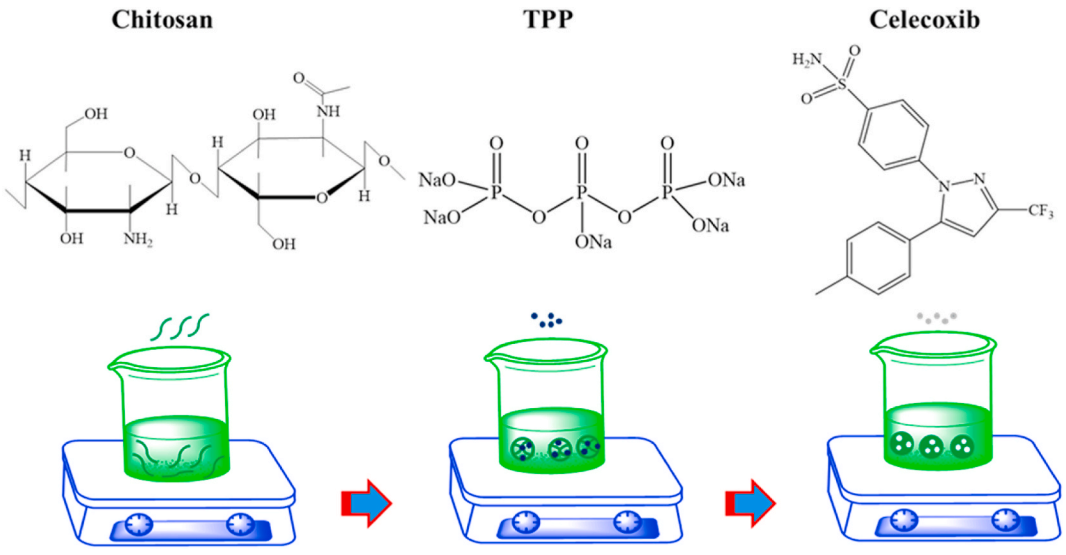

Fig. 1. Chemical structures of CS, TPP, and celecoxib, as well as the synthesis steps of CNPs.

National Cell Bank of Iran (Pasteur Institute of Iran, Tehran, Iran). Fetal Bovine Serum (FBS), Dulbecco's modified Eagle's medium (DMEM)/Ham's F12 medium, and penicillin/streptomycin were obtained from Gibco (UK).

2.2. Preparation of celecoxib-loaded nanoparticles (CNPs)

CNPs were synthesized based on the ionic gelation of CS with TPP according to the method previously reported [17,20], with some modifications (Fig. 1). Under magnetic stirring (800 rpm) at room temperature overnight, 20 mg of CS was dissolved in 1% acetic acid (v/v, 10 mL), and the pH was adjusted to 5 using NaOH (2 M, ≤100 μL). Then, the solution was filtered using a 0.45 μm filter (Millipore, PES Membrane) to remove any possible insoluble CS. A 0.1% (w/v) solution of TPP was prepared by dissolving it in distilled water, and the pH was adjusted to 4 using a 1% (v/v) aqueous solution of acetic acid. This solution was subsequently passed through a 0.22 μm filter (Millipore). The TPP solution was added drop by drop to the CS solution under stirring. After 20 min, a celecoxib solution (1 mL) at a concentration of 3 mg/mL, prepared in ethanol, was added drop by drop to the milky suspension of NPs under stirring [17]. After 1 h, the mixture was centrifuged at 12,000 rpm (15 min, 4 °C), and the sediment was washed twice with distilled water and centrifuged again. Finally, the sediment was resuspended in distilled water and lyophilized to obtain CNPs, while the supernatant was collected to evaluate EE. Free celecoxib in the supernatant was determined by measuring the absorbance at 354 nm using an ultraviolet-visible (UV–vis) spectrophotometer and calculated using a standard calibration curve. The percentage of EE was then calculated using equation (1) [14]. Meanwhile, blank nanoparticles (BNPs) were synthesized using the same method but without adding the drug.

$$EE\ (\%) = \left(\frac{Total\ drug - Free\ drug}{Total\ drug}\right) \times 100 \quad (1)$$

2.3. Synthesis of KGN conjugated chitosan (K-CS)

CS (40 mg) was dissolved in 10 mL of a 1% (v/v) acetic acid solution overnight. After dissolution, the pH of the solution was adjusted to 5.7 using 2 M NaOH and then filtered. The EDC/NHS mixture solution (EDC, 3 mg, 0.0157 mmol, and NHS, 2 mg, 0.018 mmol) was prepared in a 0.05 M buffer of 2-morpholinoethane sulfonic acid (MES buffer, pH 5.7). KGN (2 mg, 0.006 mmol in 2 mL of ethanol) was immersed in a mixture of EDC and NHS for 12 min at room temperature. The CS solution was then reacted with the NHS-esterified KGN for 24 h under low-speed stirring. The amount of KGN utilized for the cross-link formation was 5% of the weight ratio to CS. The K-CS was then dialyzed against deionized water using a dialysis bag (Cut-off = 12–14 kDa) for one day (Fig. 2A). The conjugates were then lyophilized for future use. The amount of free KGN in deionized water after dialysis was also determined to calculate CE [6] using UV–vis spectrophotometry at 289 nm. The percentage of CE was then calculated using equation (2) [6].

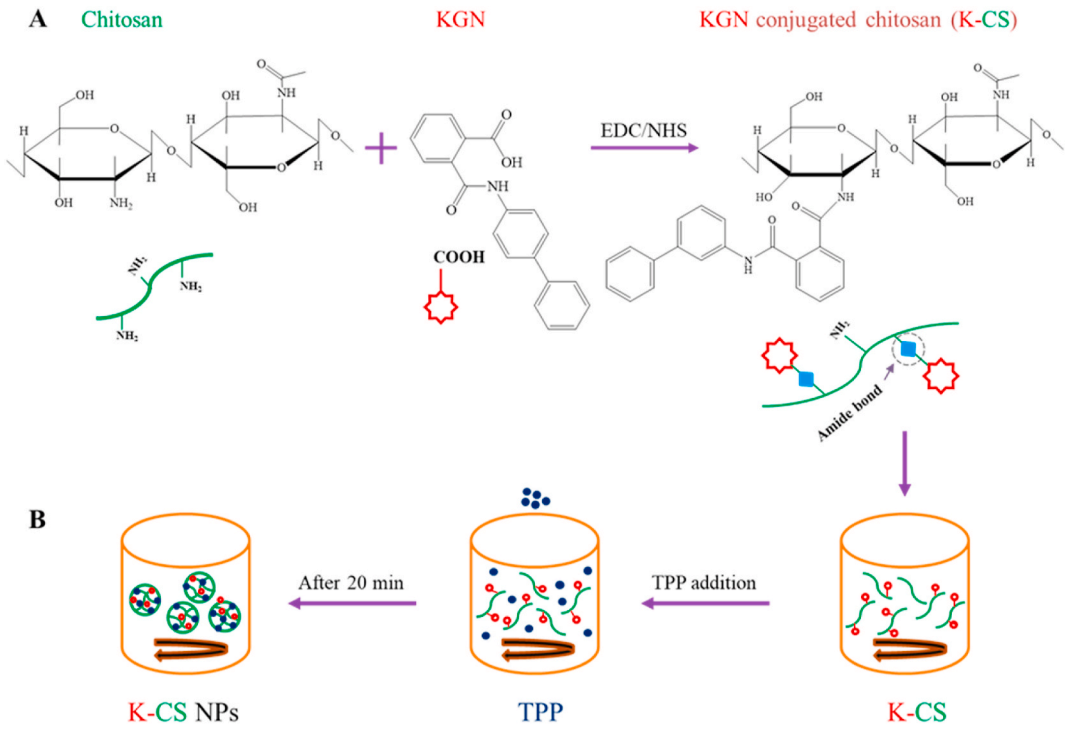

Fig. 2. The chemistry involved in the conjugation of CS and KGN (K-CS) (A) and the synthesis steps of K-CS NPs (B).

$$\text{CE}\ \ (\%) = \left(\frac{Total\ KGN - Unconjugated\ KGN}{Total\ KGN}\right) \times 100 \quad (2)$$

2.4. Preparation of NPs with K-CS (K-CS NPs)

K-CS NPs were synthesized based on the manufacturing method of BNPs, except that a K-CS solution was used instead of a CS solution (Fig. 2B). Briefly, KGN conjugated chitosan (K-CS) (0.2%, w/v) was dissolved in 10 mL of 1% acetic acid, and the pH was adjusted to 5 using NaOH (2 M, ≤100 μL). Then, TPP solution (0.1%, w/v, 4 mL) was added to the K-CS solution. After 20 min, the resulting milky suspension was centrifuged at 12000 rpm for 15 min and washed twice with deionized water. Finally, K-CS NPs were resuspended in distilled water and lyophilized for future use. The physical conditions used to produce K-CS NPs are shown in Table S1.

2.5. Characterization of CNPs, K-CS, and K-CS NPs

FT-IR (Fourier-Transform Infrared Spectroscopy) analysis was utilized to determine the surface chemistry of the synthesized K-CS conjugate and confirm the formation of CNPs and K-CS NPs (model FT-IR-8400s, Shimadzu Corp, Kyoto, Japan). The lyophilized powders of K-CS conjugate, K-CS NPs, and CNPs were mixed with KBr and compressed into a pellet using a hydraulic press. The FT-IR spectra were recorded between 4000 and 400 cm^{-1}.

2.6. Determination of particle size, PDI, and zeta potential

The physicochemical properties of NPs, including particle size, PDI, and zeta potential, were analyzed using a Zetasizer Nano ZS from Malvern Instruments (Malvern, UK) at 25 °C after dilution with deionized water. The experiments were carried out in triplicate, and all the data were reported as the means ± standard deviation (SD).

2.7. Morphology determination

The surface morphology of CNPs and K-CS NPs was examined using atomic force microscopy (AFM, Shimadzu, Japan) and scanning electron microscopy (SEM, TESCAN MIRA III, Czech Republic). The image measurement of AFM was performed using a silica carbide probe. A drop of the diluted suspension of the NPs was placed on the surface of the freshly cleaved clean glass, spread out, and dried at 25 °C. For SEM, the suspensions of NPs were spread out on a glass plate and allowed to dry at room temperature. The samples were then coated with gold metal and examined.

2.8. In vitro release study

For the *in vitro* release study, the lyophilized powders of CNPs (10 mg) and K-CS NPS (20 mg) containing a specified quantity of drug were separately transferred to a dialysis bag (Cut-off = 12–14 kDa) with PBS solution [21]. Then, dialysis bags were placed in a flask containing 40 mL of PBS solution with pH 6 (pH of the inflamed joint) [22] to create sink conditions and shaken at 100 rpm at 37 °C. At different intervals, 1 mL of the release media was withdrawn for analysis and replaced with the same volume of fresh buffer (37 °C). The absorbance of the withdrawn samples was determined using a UV–vis spectrophotometer at 254 and 289 nm for celecoxib and KGN, respectively. Then, the drug concentrations were determined using the standard calibration curves for KGN ($y = 0.0487x + 0.005$, $R^2 = 0.9997$) and celecoxib ($y = 0.0542x - 0.0016$, $R^2 = 0.9995$). Equations (3) and (4) were used to calculate the amount of released drug and cumulative release (%), respectively [23]. In equation (4), Pt represents the percentage of released drug at time t and P (t-1) is the percentage of the released drug before "t". The experiments were performed in triplicate to ensure accuracy.

Amount of released drug = Concentration × dissolution bath volume × dilution factor (3)

$$\text{Cumulative release}\ (\%) = \left(\frac{Volume\ of\ sample\ withdrawn\ (mL)}{Bath\ volume\ (ml)} \times P\ (t-1)\ \right) + Pt \quad (4)$$

2.9. Cytocompatibility assay

The cytocompatibility of CNPs and K-CS NPs on human chondrocyte cells was assessed using the MTT assay [14]. Briefly, 6000 cells/well were seeded into 96-well plates in 100 μL of DMEM/F12 media supplemented with 10% FBS. After 24 h, the media were completely withdrawn and replaced with fresh medium containing various concentrations of CNPs or K-CS NPs. After 48 h, the medium was removed, and the wells were rinsed with PBS buffer (pH 7.4). Then, 10 μL of MTT solution (5 mg/mL, in PBS) was added to each well containing 90 μL of culture medium without FBS. The mixture was then incubated for 3 h at 37 °C with 5% CO_2. The MTT solution was removed, and 100 μL of DMSO was added to dissolve the formazan crystals. Then, the optical density of the formazan product was measured at 570 nm using a microplate reader (Synergy H1MFD, BioTek Instruments, USA). Cell viability was calculated using equation (5) [14].

$$\text{Viability\%} = \left(\frac{Mean\ OD\ of\ sample}{Mean\ OD\ of\ control}\right) \times 100 \quad (5)$$

2.10. Blood compatibility assay

A hemolytic test was performed to assess the hemocompatibility of NPs by measuring the percentage of hemolysis [14]. After obtaining institutional ethical approval and informed consent, fresh blood from a healthy volunteer was centrifuged at 3600 rpm (10 min). After being separated from plasma, red blood cells (RBCs) were rinsed three times with PBS (pH 7.4). Then, the determined concentrations of freeze-dried NPs were incubated with RBC suspension in a 96-well plate (three repetitions) at 37 °C for 1 h. RBC suspensions incubated with a 0.9% saline solution (lysis ~0%) and 1% Triton X-100 solution (lysis ~100%) were considered as the negative control and positive control, respectively [24]. After incubation, the mixtures were centrifuged at 3600 rpm (10 min) and the absorbance of the supernatant at 414 nm, the maximum absorbance of hemoglobin, was determined by photometric analysis. The hemolysis ratio was calculated using the following formula [14,24].

$$\text{Hemolysis\%} = \left(\frac{\textit{Mean OD of sample} - \textit{Mean OD of negative control}}{\textit{Mean OD of positive control} - \textit{Mean OD of negative control}}\right) \times 100 \quad (6)$$

2.11. The IL-1β-stimulated human chondrocytes

IL-1β, a crucial inflammatory cytokine, was incubated with seeded chondrocyte cells to simulate a pro-inflammatory environment as an *in vitro* model of OA [8,25]. After a 5 h incubation with IL-1β (10 ng/mL) [8,26], cells were treated with CNPs and K-CS NPs, alone or in combination, for 48 h to investigate their impact on the mRNA expression of inflammatory and cartilage-related genes in OA cells.

2.12. RNA isolation and qRT-PCR

Real-time PCR was used to monitor changes in the expression level of the target genes. RNA was extracted from the treated cells using the TRIzol reagent. The extracted RNA was quantitatively evaluated using a Thermo Scientific NanoDrop device. A cDNA synthesis kit (Thermo Scientific RevertAid First Strand cDNA Synthesis Kit) was utilized to reverse-transcribe the total RNA. Finally, real-time RT-PCR was utilized to assess the effects of CNPs and K-CS NPs on inflammatory and cartilage marker gene expressions, such as TNF-α, COX-2, collagen-II (COL2A1), and SOX-9. The reaction contained 10 μL of SYBR Green Master Mix, 9 μL of diluted cDNA, 0.5 μL of forward primer, and 0.5 μL of reverse primer. The reaction mix was incubated for 10 min at 95 °C, followed by 40 cycles of 15 s at 95 °C, 30 s at 60 °C and 30 s at 72 °C. The target mRNA expression level was calculated using the $2^{-(\Delta\Delta CT)}$ method and GAPDH (glyceraldehyde 3-phosphate dehydrogenase) was utilized as the reference gene. The specific primers used to amplify the desired genes are listed in Table S2.

2.13. Statistics

All experiments were performed three times and analyzed using one-way analysis of variance (ANOVA) with GraphPad Prism (version 8.0.2.263). The results were expressed as the means ± SD. A p-value <0.05 (*) was considered statistically significant.

3. Results and discussion

We had initially attempted to load celecoxib on K-CS NPs. The EE% of celecoxib on K-CS NPs was low (17 ± 1.3). Consequently, we opted to load KGN and celecoxib separately into different CS NPs. Celecoxib was loaded onto the surface of formed NPs (CNPs) to enable immediate release. Meanwhile, KGN was covalently attached to the CS polymer (K-CS) to improve its solubility and prolong its release. Then, K-CS NPs were synthesized using K-CS. In the next step, we investigated the potential chondroprotective and anti-inflammatory effects of these compounds, individually or in combination, in an *in vitro* model of OA.

3.1. Synthesis of K-CS, K-CS NPs and CNPs

Entrapment of drugs inside NPs can prevent their degradation in harsh conditions, increase the solubility of hydrophobic drugs, improve the bioavailability of the drug, facilitate drug delivery to the target site, and control their release [27]. There are several ways to integrate drugs into NPs, including (A) the covalent linkage between the polymer matrix and drugs [6], (B) drug adsorption on the surface of NPs (adsorption method) [17], and (C) the physical entrapment of drugs during nanoparticle synthesis (incorporation method) [14,20,27,28]. Glutaraldehyde, a chemical cross-linking agent, has toxic effects, while TPP is a non-toxic ionic cross-linking agent popular for preparing reproducible CS NPs. Carbodiimide chemistry, a common technique to covalently link ligands, is typically employed to form an amide bond between an amine and carboxylic group [6]. Covalent attachment of a drug to a hydrophilic polymer can increase the aqueous solubility of hydrophobic drugs, thereby altering the pharmacokinetics and biodistribution of the drug in the body [6,29]. Therefore, in this study, the carboxyl group of KGN was covalently attached to the amine group of CS using EDC/NHS as a catalytic system to increase its solubility and control its release. The chemistry involved in the conjugation of CS and KGN is shown in Fig. 2A. The K-CS NPs were synthesized by the interaction between the remaining amine groups in K-CS and anion groups in a polyanion molecule (TPP). In this study, CNPs were prepared using the adsorption method to expedite release, where celecoxib was adsorbed on the surface of the formed NPs. To create the $-NH_3^+$ site, the pH of the CS solution was adjusted to 5 [30]. When TPP is

dissolved in deionized water, the OH^- and $P_3O_{10}^{5-}$ ions, which can compete to react with $-NH_3^+$ in the CS polymer, are simultaneously produced in the TPP solution [30]. In this research, to facilitate the crosslinking of the $-NH_3^+$ sites on CS with $P_3O_{10}^{5-}$ ions, the pH of the TPP solution was adjusted to 4 to ensure that only $P_3O_{10}^{5-}$ ions were present in the solution. The NPs formed after adding TPP were freeze-dried and stored at 4 °C to perform the subsequent tests.

3.2. Analysis of size and morphology of K-CS NPs and CNPs

Some characteristics of nanoparticle systems, such as drug release and the stability of drug-loaded NPs, are affected by the morphology, size, and distribution of NPs [28]. The images obtained from AFM and SEM microscopes clearly show that both CNPs and K-CS NPs are spherical (Fig. S1), which is consistent with other reports [6,31–34]. Since the size of NPs in a dry form differs from that in a form dispersed in water, it was evaluated only by DLS, which has a liquid environment similar to the body. The surface charge and PDI of the K-CS NPs and CNPs in the aqueous medium were determined using DLS. The CNPs and K-CS NPs had an average size of 352.6 ± 22.5 nm and 232.7 ± 4.5 nm, respectively, while BNPs had an average size of 214.3 ± 4.6 nm (Table 1). Also, while the BNPs had a zeta potential of +35.7 ± 0.8 mV (Fig. 3A), the zeta potential of the CNPs (Fig. 3B) and K-CS NPs (Fig. 3C) was +50.4 ± 1.5 mV and +17.5 ± 1.6, respectively. Due to the cationic nature of CS, the zeta potential of NPs was positive. However, the covalent attachment of the carboxyl group of KGN to the amine group of CS decreased the number of amine groups on the CS polymer. As a result, the zeta potential of K-CS NPs decreased compared to BNPs (Table 1). Loading celecoxib onto the formed NPs resulted in increased particle size and zeta potential compared to BNPs. The increase in zeta potential can be attributed to $-NH_2$ groups present in celecoxib. Considering that there is no limit on the average diameter of the particles delivered to the knee joint, nowadays hydrogels, microparticles, and NPs are used to improve the delivery of drugs into the knee joint [3]. Therefore, the size of NPs synthesized in this study may be suitable for IA injection. However, there is still no consensus on the most appropriate size of drug formulations for IA injection [6]. While Eswaramoorthy et al. recommended a size of about 51–85 μm for IA injection [35], another study suggested NPs smaller than 60 nm for injection [36]. In this regard, Kang et al. injected two particles with different sizes (NPs and microparticles) into the joint cavity of the rat OA model to investigate the optimal size for IA drug delivery [6]. The results did not show a significant difference between the two different sizes [6]. The PDI of BNPs, K-CS NPs, and CNPs were 0.202 ± 0.001, 0.24 ± 0.01, and 0.37 ± 0.02, respectively. The results were in line with other reports [37,38]. A PDI below 0.5 indicates that NPs have a monodisperse distribution [37–39].

3.3. Calculation of EE and CE

The drug loading method, the physical and chemical properties of the drug, the concentration of the polymer and the drug, and the contact time of the drug with the polymer affect the percentage of EE and CE of the formulation [27]. To minimize the amount of injected formulation, the percentage of EE and CE should be high [27]. The quantity of celecoxib loaded on CNPs was determined by analyzing the free celecoxib in the supernatant of CNPs using a spectrophotometer at 254 nm. The CNPs prepared using the adsorption method resulted in NPs with a high percentage of EE. The EE percentage of CNPs was consistent with the efficiency values reported by other researchers for encapsulating hydrophobic molecules in CS NPs [32,33,40]. The binding efficiency of KGN to CS (CE%) in K-CS was 70.5 ± 2.2%, indicating that more than 50% of KGN was conjugated to CS (Table 1).

3.4. FT-IR analysis of K-CS, K-CS NPs and CNPs

The formation of NPs was confirmed by analyzing the functional groups in their FT-IR spectra (Fig. 4). The peaks at 1591 and 1087 cm^{-1} are attributed to the N–H bending (amine and amide II) and C–O stretching vibration, respectively, in the CS spectrum [31]. The interaction of CS with TPP translocated these peaks to 1531 and 1074 cm^{-1} in the BNPs spectrum, respectively [31]. The peak related to the stretching vibration of –OH and $-NH_2$ groups (3425 cm^{-1}) was broadened in the BNPs spectrum due to the interaction of the NH_2 group of CS with the phosphate groups of TPP and the increase in hydrogen bonding. Moreover, a more pronounced variation in the peak was observed following loading with celecoxib. This peak was flattened in CNPs compared to BNPs, likely due to the interactions of celecoxib with the non-cross-linked amino groups in CS. In the celecoxib spectrum, the peaks displayed as a double at 3344 and 3224 cm^{-1} are related to the N–H stretching vibration of the $-SO_2NH_2$ group [41]. The bands at 1164 and 1348 cm^{-1} are related to S═O symmetric and asymmetric stretching, respectively [41], which are also observed in the CNPs spectrum. Therefore, it was confirmed that celecoxib was adsorbed on CNPs. The FT-IR spectrum also confirmed the formation of an amide linkage between KGN and CS (Fig. 4B). In the KGN spectrum, the peaks at 3031 and 1718 cm^{-1} are attributed to aromatic C–H and C═O stretching, respectively [29]. The absorption peak at 3031 cm^{-1} corresponding to the aromatic C–H bond in pure KGN shifted to 3028 cm^{-1} in the FT-IR pattern of K-CS. The adsorption peaks at 1650 and 1591 cm^{-1} in the CS spectrum are related to the C═O stretching in the amide group and the N–H bending from amine and amide II, respectively [31]. The intensity of peaks at 1650 and 1591 cm^{-1} (CS) increased

Table 1
DLS measurements of NPs, including size, zeta potential, and PDI, as well as the percent of EE and CE.

NP name	Size (nm)	PDI	Zeta potential (mV)	EE (%)	CE (%)
BNPs	214.3 ± 0.46	0.202 ± 0.001	35.7 ± 0.8	–	–
K-CS NPs	232.7 ± 4.5	0.24 ± 0.01	17.5 ± 1.6	–	70.5 ± 2.2
CNPs	352.6 ± 22.5	0.37 ± 0.02	50.4 ± 1.5	95.8 ± 0.9	–

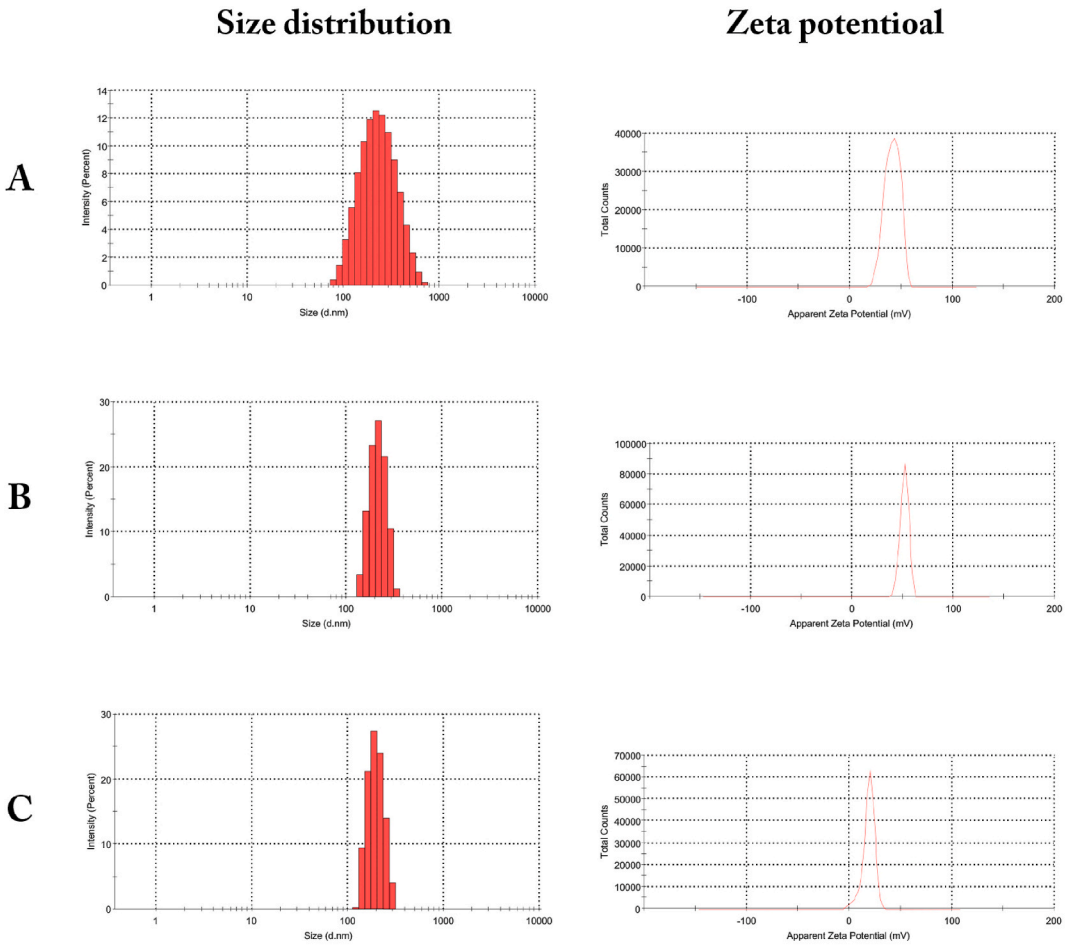

Fig. 3. Characteristics of NPs: Size distribution and zeta potential of (A) BNPs, (B) CNPs, and (C) K-CS NPs.

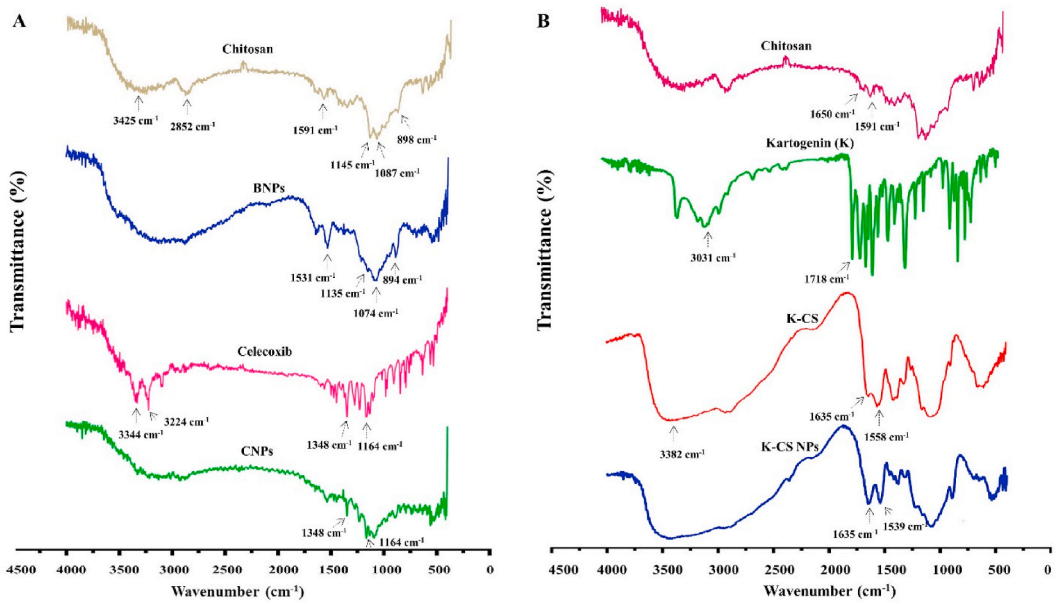

Fig. 4. FT-IR spectra of CS, BNPs, Celecoxib, and CNPs (A) and the FT-IR spectra of CS, KGN, K-CS, and K-CS NPs (B).

and shifted to 1635 and 1558 cm^{-1} in the spectrum of K-CS, confirming the formation of the amide bond between the carboxyl groups of KGN and the amine groups of CS [6]. Although there are similarities between the spectra of K-CS and K-CS NPs, there are also differences (Fig. 4B). Owing to the interaction of the phosphate groups of TPP with the $–NH_2$ groups of K-CS and the increase in hydrogen bonding, the peak at 3382 cm^{-1}, which was related to the stretching vibration of $–NH_2$ and –OH groups in the K-CS spectrum, was broadened in the K-CS NPs spectrum. The intensity of the peak at 1635 cm^{-1} (K-CS) was enhanced and remained the same (1635 cm^{-1}) in the spectrum of K-CS NPs, but the peak at 1558 cm^{-1} shifted to 1539 cm^{-1}. In conclusion, the results indicate that BNPs, K-CS NPs, and CNPs have been successfully prepared using an ionic gelation method.

3.5. *In vitro release study*

Fig. 5A and B show the release of KGN and celecoxib from K-CS NPs and CNPs *in vitro*, respectively. Factors such as particle size, hydrophilicity or hydrophobicity of the polymer and drug, functional groups of the drug, the molecular weight of the drug and polymer, and the type of linkage between them can affect the drug release rate from NPs [29,42]. The release of KGN from K-CS NPs continued for more than two weeks because the covalent bonds between the drug and CS were stronger than ionic bonds. Meanwhile, the entanglement of CS chains with KGN protected the covalent linkage [6] between CS and KGN in K-CS NPs, resulting in sustained release. Although the release profile of KGN from K-CS NPs was continuous, a small amount of the drug was detected after two weeks. This result was consistent with the release profile described by Kang et al. [6]. They reported that the cumulative release of KGN after 7 weeks was about 35% [6]. Due to shaking conditions and warm temperatures, more KGN was likely released and degraded in the PBS solution [6]. The release of celecoxib from CNPs exhibited a biphasic pattern, characterized by a rapid burst release followed by a slow and sustained release (plateau step). Electrostatic bonds, such as hydrogen bonds and van der Waals forces, are weaker than covalent bonds. The initial burst release is probably caused by the release of drugs that were weakly attached to the surface of CNPs. The rapid release of a significant amount of celecoxib from CNPs can enable the drug to rapidly reach curative levels to manage pain and suppress the symptoms of inflammatory diseases such as OA [39]. In general, around 34% of celecoxib loaded in CNPs was released in the first hour, and then it provided a continuous release of celecoxib for up to 48 h. The slow release may be due to drug diffusion from the CNPs matrix. The release pattern of celecoxib from CS NPs was similar to the results of other studies [29,34,43,44].

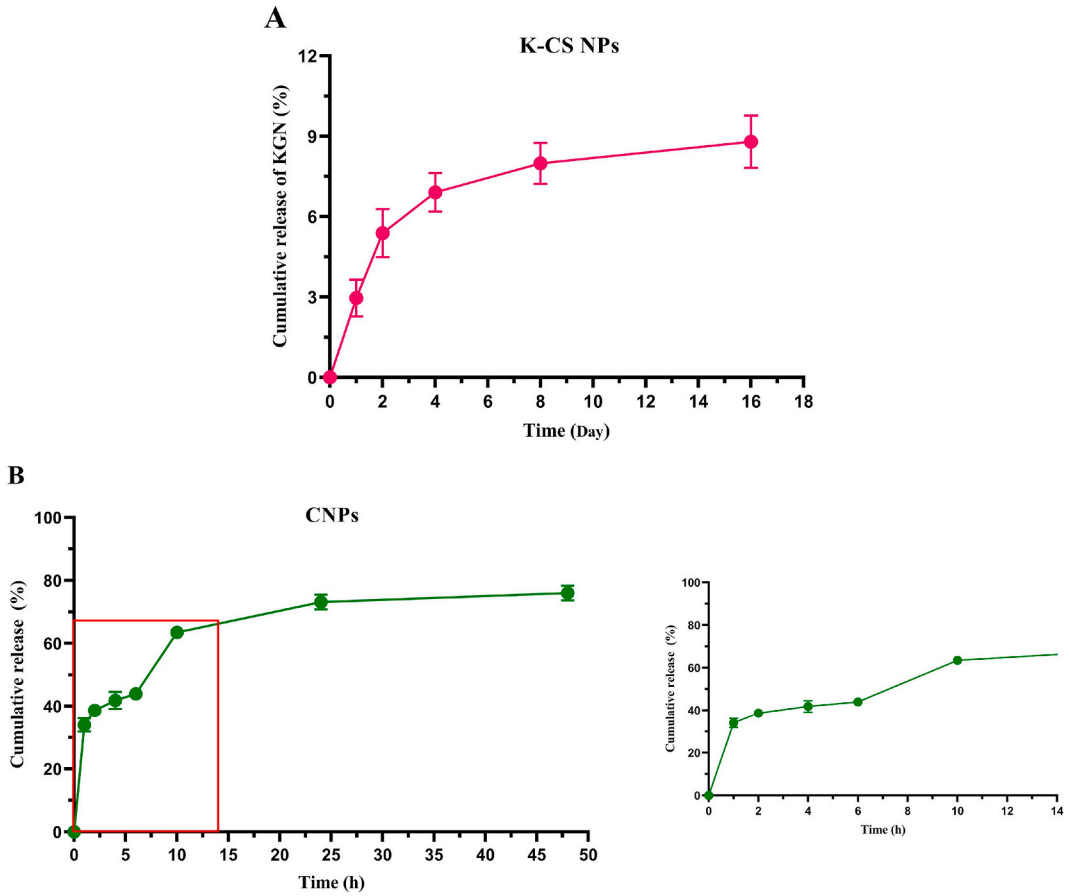

Fig. 5. The *in vitro* release of KGN from K-CS NPs (A) and celecoxib from CNPs (B) in PBS solution.

3.6. Effect of CNPs and K-CS NPs on human chondrocyte viability

To confirm whether this drug delivery system is safe for chondrocytes, it is necessary first to investigate the toxicity of BNPs. Therefore, the cytotoxicity of BNPs on human chondrocytes was analyzed using the MTT assay. A certain concentration of BNPs (40 μg/mL to 1.6 mg/mL) was used to study their potential cytotoxicity. The results showed that the cell viability of chondrocytes was not affected up to 1.6 mg/mL after 48 h of incubation. No significant difference was observed between the groups and compared to 0 concentration (control group) for BNPs (Fig. 6A). This result confirmed the safety of this system. It aligned with other reports [14,27,45,46]. Based on the results of EE and CE% of CNPs and K-CS NPs, respectively, a large amount of drug was loaded on NPs. The higher the amount of drug loading in NPs, it can decrease the frequency of injections [14]. However, high drug loading can be toxic in monolayer cultures. Therefore, the different concentrations of K-CS NPs and CNPs were prepared, and their potential cytotoxicity on chondrocytes were investigated by MTT test to find a concentration that is not toxic in monolayer culture. The results showed that cell viability was not affected by K-CS NPs and CNPs at concentrations up to 50 and 25 μg/mL, respectively, after 48 h of incubation (Fig. 6B and C). As a result, the concentrations of 0.025 and 0.05 mg/mL were selected for CNPs and K-CS NPs, respectively, to use in subsequent studies.

3.7. Hemocompatibility assay

The characteristics of NPs, such as size, shape, surface charge, and chemical composition, can affect the membrane integrity of RBCs [24]. NPS shouldn't interact with components in the blood. Therefore, the blood compatibility of BNPs, K-CS NPs, and CNPs was evaluated using the hemolytic test at a given concentration range (15.625–1000 μg/mL). The results (Fig. 7) indicated that the hemolysis rate of NPs was lower than 5%, a safety crucial value [28,47,48]. In the 15.625–1000 μg/mL range, the highest amount of hemolysis for BNPs, K-CS NPs, and CNPs was 0.64, 1.22, and 2.85%, respectively. The higher hemolysis percentage of CNPs in the 1 mg/mL concentration compared to BNPs and K-CS NPs is probably due to SO_2NH_2 groups of celecoxib [49]. Ultimately, the results showed minimal damage caused by BNPs, K-CS NPs, and CNPs to RBCs, and they have good hemocompatibility. Investigation of blood compatibility of CS NPs synthesized using the ionic gelation method by Nadesh et al. showed that the solvent type used to disperse CS NPs affects their hemocompatibility [50]. CS NPs dispersed in solvents such as saline, lactic acid, and PBS buffer have satisfactory hemocompatibility compared to acetic acid solution [14,27,50]. Our result was in line with this study [50].

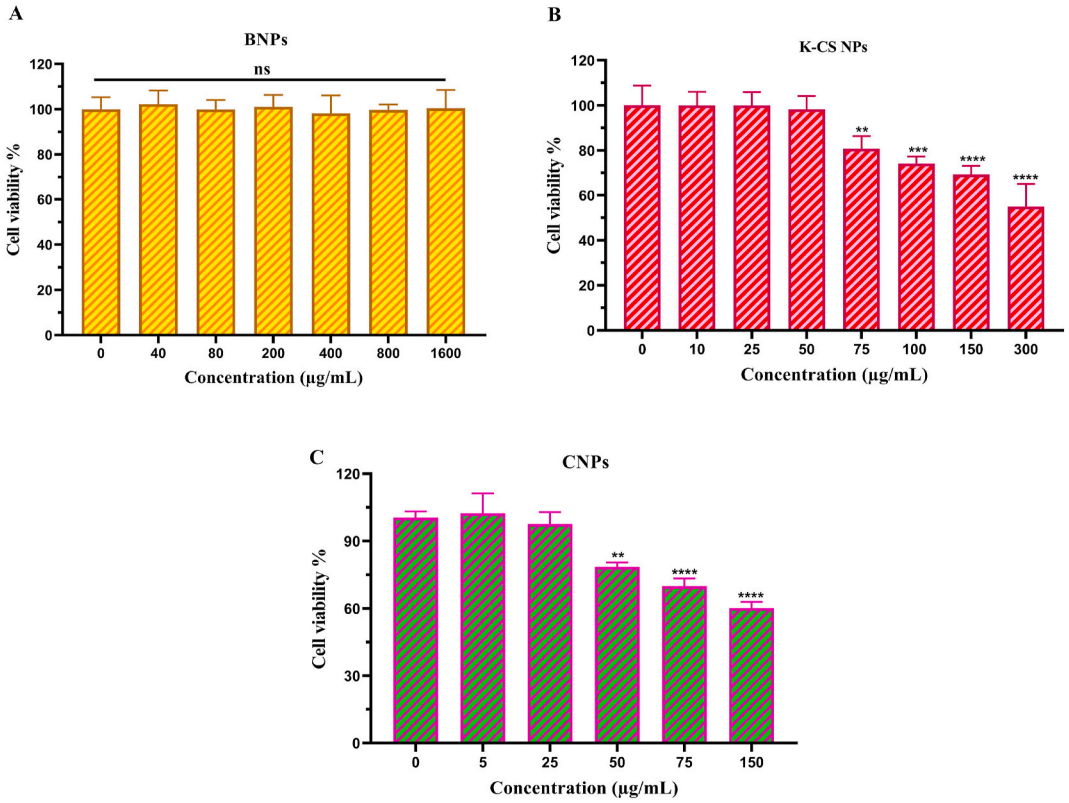

Fig. 6. Cytotoxicity assay of NPs using chondrocytes after incubation (48 h) with BNPs (A), K-CS NPs (B), and CNPs (C) at various concentrations. **p < 0.01, ***p < 0.001, ****p < 0.0001 versus control group (0 concentration). ns: not significant.

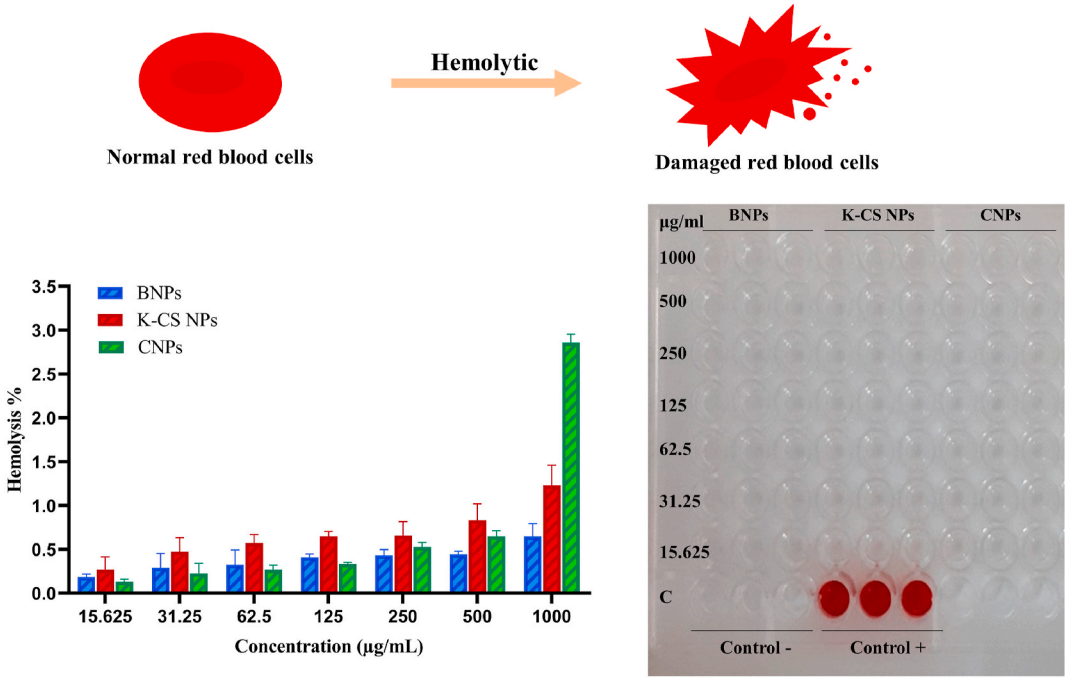

Fig. 7. Evaluation of hemolysis assay of BNPs, K-CS NPs, and CNPs at a given concentration range (15.625–1000 µg/mL). 0.9% saline solution (0% lysis) and 1% Triton X-100 (100% lysis) were used as negative and positive controls, respectively.

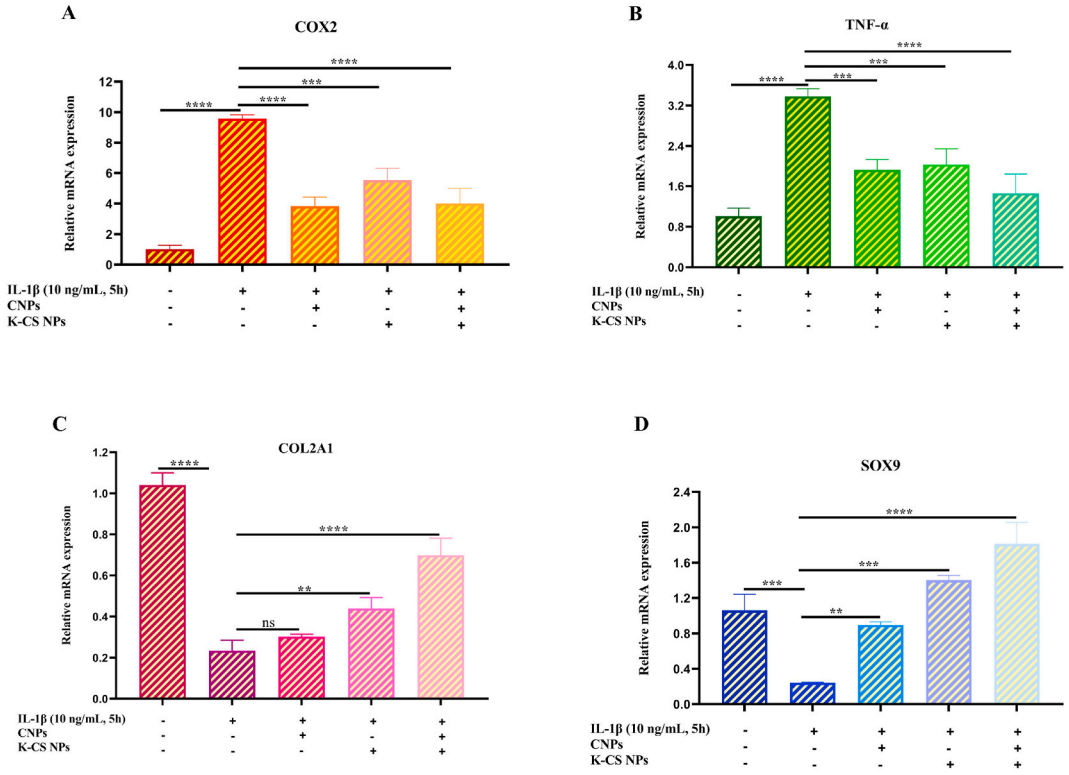

Fig. 8. Effect of CNPs and K-CS NPs, individually or in combination , on the mRNA expression of COX-2 (A), TNF-α (B), COL2A1 (C), and SOX-9 (D) in IL-1β pretreated human chondrocytes. **p < 0.01, ***p < 0.001, ****p < 0.0001. ns: not significant. The values are shown as mean ± SD (n = 3).

3.8. Effect of CNPs and K-CS NPs on gene expression

The cells were cultured in DMEM/F12 media and pre-treated for 5 h with IL-1β to mimic an *in vitro* model of OA [8], and then treated for 48 h with CNPs and K-CS NPs, at the concentration of 25 and 50 μM, respectively, alone or in combination with each other. Then, the analysis of gene expression of some genes such as TNF-α, COX-2, COL2A1, and SOX9 was evaluated by qRT-PCR. Many studies exhibited that stimulation of chondrocytes with IL-1β caused a remarkable up-regulation of inflammatory genes (TNF-α, COX-2, and IL-6) and a considerable down-regulation of cartilage-related genes such as SOX9, aggrecan, and COL2A1 [2,8,51]. Cyclooxygenase-2 (COX-2) enzyme, one of the inflammatory mediators, regulates the expression of prostaglandin E2 (PGE2), which causes pain and swelling during inflammation [7,52]. Selective blocking of this enzyme by celecoxib as a COX-2 inhibitor can slow the progression of OA. Cells stimulated with IL-1β showed a remarkable increase in COX-2 mRNA expression compared to the control group (Fig. 8A), consistent with other reports [2,8]. While treatment with CNPs or K-CS NPs decreased its expression in human chondrocytes stimulated with IL-1β (Fig. 8A). CNPs inhibited COX-2 mRNA expression better than K-CS NPs due to having celecoxib, a specific COX-2 inhibitor (Fig. 8A) [8]. One of the main inflammatory chemokines is TNF-α, which plays a key role in maintaining inflammation by activating macrophages [2]. While TNF-α mRNA expression level was increased in chondrocytes stimulated with IL-1β, treatment with CNPs or K-CS NPs decreased the effect of IL-1β on its expression (Fig. 8B). Also, the combination of both NPs increasingly inhibited the impact of IL-1β on TNF-α mRNA expression in IL-1β-stimulated chondrocytes (Fig. 8B). COL2A1 is one of the main components of cartilage ECM, whose expression is positively regulated by a transcription factor called SOX-9 [6]. Pretreatment of cells with IL-1β significantly decreased COL2A1 and SOX-9 mRNA expression compared with the untreated group (Fig. 8C and D). Treatment with CNPs alone showed no detectable change in COL2A1 mRNA expression, while SOX-9 mRNA expression was increased (Fig. 8C and D). The incubation with K-CS NPs alone counteracted the negative effect of IL-1β on mRNA expression of COL2A1 and SOX-9 in IL-1β-stimulated chondrocytes. However, the combination of CNPs and K-CS NPs increasingly inhibited the impact of IL-1β on mRNA expression of COL2A1 and SOX-9 in IL-1β-stimulated chondrocytes compared to that observed by either treatment alone (Fig. 8C and D). In general, our results showed that treatment of IL-1β-pretreated chondrocytes with CNPs or K-CS NPs remarkably limited the negative effect of IL-1β, especially when both NPs were combined.

4. Conclusions

The conjugation of CS and KGN was carried out successfully by an EDC/NHS as a catalytic system and confirmed by FT-IR spectroscopy. Then, K-CS NPs and CNPs were successfully prepared by different methods using an ionic gelation method. Since there is no limit to the average diameter of NPs injected into the knee cavity, the size of both NPs could be suitable for IA injection. Based on hemolysis results, they also showed good hemocompatibility. Also, *in vitro* results showed that treatment of IL-1β-pretreated cells with CNPs or K-CS NPs remarkably limited the negative effect of IL-1β, especially when both NPs were surveyed in combination. However, further investigations using an animal model of OA are needed to prove whether the simultaneous application of CNPs and K-CS NPs can rapidly suppress inflammation and pain and regenerate cartilage.

Ethics statement

The study was approved (Approval Number: IR.SEMUMS.REC.1398.284) by the Ethics Committee of Semnan University of Medical Sciences, Semnan, Iran. All methods were performed under the relevant guidelines and regulations. The study was conducted according to local legislation and institutional requirements.

Funding

This research was supported by a grant from Semnan University of Medical Sciences, Semnan, Iran (grant number 1667).

Consent for publication

All authors have read and approved the final version of the manuscript.

Data availability statement

The corresponding author (DN) will make raw data available on request.

CRediT authorship contribution statement

Zahra Nabizadeh: Writing – original draft, Visualization, Validation, Project administration, Methodology, Investigation, Formal analysis, Data curation, Conceptualization. **Mahmoud Nasrollahzadeh:** Writing – review & editing, Validation, Methodology, Investigation, Data curation. **Benjamin Kruppke:** Writing – review & editing, Validation. **Davood Nasrabadi:** Validation, Supervision, Funding acquisition.

Declaration of competing interest

The authors declare that they have no known competing financial interests or personal relationships that could have appeared to influence the work reported in this paper.

Acknowledgments

We appreciate the support of the Iran Nanotechnology Innovation Council (INIC), the University of Qom, TU Dresden, and the Semnan University of Medical Sciences. The authors thank Dr. Fatemeh Ahmadpoor for her scientific comments. We are also grateful to Mr. Ali Heydarian for providing DLS facilities.

Appendix A. Supplementary data

Supplementary data to this article can be found online at https://doi.org/10.1016/j.heliyon.2024.e31058.

References

[1] R.H. Koh, Y. Jin, J. Kim, N.S. Hwang, Inflammation-modulating hydrogels for osteoarthritis cartilage tissue engineering, Cells 9(2) (2020) 419.
[2] W. Zheng, Z. Feng, S. You, H. Zhang, Z. Tao, Q. Wang, H. Chen, Y. Wu, Fisetin inhibits IL-1β-induced inflammatory response in human osteoarthritis chondrocytes through activating SIRT1 and attenuates the progression of osteoarthritis in mice, Int. Immunopharm. 45 (2017) 135–147.
[3] Z. Nabizadeh, M. Nasrollahzadeh, H. Daemi, M.B. Eslaminejad, A.A. Shabani, M. Dadashpour, M. Mirmohammadkhani, D. Nasrabadi, Micro-and nanotechnology in biomedical engineering for cartilage tissue regeneration in osteoarthritis, Beilstein J. Nanotechnol. 13 (2022) 363–389.
[4] L. Roseti, G. Desando, C. Cavallo, M. Petretta, B. Grigolo, Articular cartilage regeneration in osteoarthritis, Cells 8(11) (2019) 1305.
[5] R.I. El-Gogary, M.A. Khattab, H. Abd-Allah, Intra-articular multifunctional celecoxib loaded hyaluronan nanocapsules for the suppression of inflammation in an osteoarthritic rat model, Int. J. Pharm. 583 (2020) 119378.
[6] M.L. Kang, J.-Y. Ko, J.E. Kim, G.-I. Im, Intra-articular delivery of kartogenin-conjugated chitosan nano/microparticles for cartilage regeneration, Biomaterials 35 (37) (2014) 9984–9994.
[7] A.R. Tellegen, I. Rudnik-Jansen, B. Pouran, H.M. De Visser, H.H. Weinans, R.E. Thomas, M.J.L. Kik, G.C.M Grinwis, J.C. Thies, N. Woike, Mihov G., Emans P.J., Meij B.P., Creemers, L.B., Tryfonidou, M.A., Controlled release of celecoxib inhibits inflammation, bone cysts and osteophyte formation in a preclinical model of osteoarthritis, Drug Deliv. 25(1) (2018) 1438–1447.
[8] S. Cheleschi, S. Tenti, S. Giannotti, N. Veronese, J.-Y. Reginster, A. Fioravanti, A combination of celecoxib and glucosamine sulfate has anti-inflammatory and chondroprotective effects: Results from an in vitro study on human osteoarthritic chondrocytes, Int. J. Mol. Sci. 22(16) (2021) 8980.
[9] K. Johnson, S. Zhu, M.S. Tremblay, J.N. Payette, J. Wang, L.C. Bouchez, S. Meeusen, A. Althage, C.Y. Cho, X. Wu, Schultz P.G., A stem cell–based approach to cartilage repair, Science 336 (2012) 717–721.
[10] J.C. Marini, A. Forlino, Replenishing cartilage from endogenous stem cells, N. Engl. J. Med. 366 (2012) 2522–2524.
[11] M.F. Rai, C.T. Pham, Intra-articular drug delivery systems for joint diseases, Curr. Opin. Pharmacol. 40 (2018) 67–73.
[12] W. Fan, J. Li, L. Yuan, J. Chen, Z. Wang, Y. Wang, C. Guo, X. Mo, Z. Yan, Intra-articular injection of kartogenin-conjugated polyurethane nanoparticles attenuates the progression of osteoarthritis, Drug Deliv. 25(1) (2018) 1004–1012.
[13] W. Yan, X. Xu, Q. Xu, Z. Sun, Z. Lv, R. Wu, W. Yan, Q. Jiang, D. Shi, An injectable hydrogel scaffold with kartogenin-encapsulated nanoparticles for porcine cartilage regeneration: A 12-month follow-up study, Am. J. Sports Med. 48(13) (2020) 3233–3244.
[14] Z. Nabizadeh, M. Nasrollahzadeh, A.A. Shabani, M. Mirmohammadkhani, D. Nasrabadi, Evaluation of the anti-inflammatory activity of fisetin-loaded nanoparticles in an in vitro model of osteoarthritis, Sci. Rep. 13 (2023) 15494.
[15] M. Kababian, E. Cheraghi, E. Moradi-Asl, A. Saghafipour, Z. Nabizadeh, Comparative study of physiochemical and antimicrobial properties of adult cockroaches-extracted chitosan, J. Appl. Biol. Sci. 18(1) (2024) 94–105.
[16] M. Nasrollahzadeh, M. Sajjadi, S. Iravani, R.S. Varma, Starch, cellulose, pectin, gum, alginate, chitin and chitosan derived (nano) materials for sustainable water treatment: A review, Carbohydr. Polym. 251 (2021) 116986.
[17] G.V. Kumar, S. Chia-Hung, P. Velusamy, Preparation and characterization of kanamycin-chitosan nanoparticles to improve the efficacy of antibacterial activity against nosocomial pathogens, J. Taiwan Inst. Chem. Eng. 65 (2016) 574–583.
[18] F. Canal, J. Sanchis, M.J. Vicent, Polymer–drug conjugates as nano-sized medicines, Curr. Opin. Biotechnol. 22(6) (2011) 894–900.
[19] R. Duncan, F. Spreafico, Polymer conjugates. Pharmacokinetic considerations for design and development, Clin. Pharmacokinet. 27 (1994) 290–306.
[20] Y. Zhang, Y. Yang, K. Tang, X. Hu, G. Zou, Physicochemical characterization and antioxidant activity of quercetin-loaded chitosan nanoparticles, J. Appl. Polym. Sci. 107(2) (2008) 891–897.
[21] M. Iraji, M. Salehi, R.E. Malekshah, A. Khaleghian, F. Shamsi, Liposomal formulation of new arsenic schiff base complex as drug delivery agent in the treatment of acute promyelocytic leukemia and quantum chemical and docking calculations, J. Drug Deliv. Sci. Technol. 75 (2022) 103600.
[22] T. Jin, D. Wu, X.-M. Liu, J.-T. Xu, B.-J. Ma, Y. Ji, Y.-Y. Jin, S.-Y. Wu, T. Wu, K. Ma, Intra-articular delivery of celastrol by hollow mesoporous silica nanoparticles for pH-sensitive anti-inflammatory therapy against knee osteoarthritis, J. Nanobiotechnol. 18 (2020) 94.
[23] A.R. Chandrasekaran, C.Y. Jia, C.S. Theng, T. Muniandy, S. Muralidharan, S.A. Dhanaraj, Invitro studies and evaluation of metformin marketed tablets-Malaysia, J. Appl. Pharmaceut. Sci. 01 (05) (2011) 214–217.
[24] A. Sasidharan, L.S. Panchakarla, A.R. Sadanandan, A. Ashokan, P. Chandran, C.M. Girish, D. Menon, S.V. Nair, C.N.R. Rao, M. Koyakutty, Hemocompatibility and macrophage response of pristine and functionalized graphene, Small 8(8) (2012) 1251–1263.
[25] C.I. Johnson, D.J. Argyle, D.N. Clements, In vitro models for the study of osteoarthritis, Vet. J. 209 (2016) 40–49.
[26] S.-J. Wang, J.-Z. Qin, T.-E. Zhang, C. Xia, Intra-articular injection of kartogenin-incorporated thermogel enhancing osteoarthritis treatment, Front. Chem. 7 (2019) 677.
[27] L. Bugnicourt, C. Ladavière, Interests of chitosan nanoparticles ionically cross-linked with tripolyphosphate for biomedical applications, Prog. Polym. Sci. 60 (2016) 1–17.
[28] P. Ghosh, A.S. Roy, S. Chaudhury, S.K. Jana, K. Chaudhury, S. Dasgupta, Preparation of albumin based nanoparticles for delivery of fisetin and evaluation of its cytotoxic activity, Int. J. Biol. Macromol. 86 (2016) 408–417.
[29] M.-L. Kang, J.-E. Kim, G.-I. Im, Thermoresponsive nanospheres with independent dual drug release profiles for the treatment of osteoarthritis, Acta Biomater. 39 (2016) 65–78.
[30] F.-L. Mi, S.-S. Shyu, S.-T. Lee, T.-B. Wong, Kinetic study of chitosan-tripolyphosphate complex reaction and acid-resistive properties of the chitosan-tripolyphosphate gel beads prepared by in-liquid curing method, J. Polym. Sci. B Polym. Phys. 37(14) (1999) 1551–1564.

[31] J. Antoniou, F. Liu, H. Majeed, J. Qi, W. Yokoyama, F. Zhong, Physicochemical and morphological properties of size-controlled chitosan–tripolyphosphate nanoparticles, Colloids Surf. A Physicochem. Eng. Asp. 465 (2015) 137–146.
[32] N.S. Rejinold, M. Muthunarayanan, K. Muthuchelian, K.P. Chennazhi, S.V. Nair, R. Jayakumar, Saponin-loaded chitosan nanoparticles and their cytotoxicity to cancer cell lines *in vitro*, Carbohydr. Polym. 84 (2011) 407–416.
[33] V. Arulmozhi, K. Pandian, S. Mirunalini, Ellagic acid encapsulated chitosan nanoparticles for drug delivery system in human oral cancer cell line (KB), Colloids Surf. B Biointerfaces 110 (2013) 313–320.
[34] M. Sun, Z. Deng, F. Shi, Z. Zhou, C. Jiang, Z. Xu, X. Cui, W. Li, Y. Jing, B. Han, W. Zhang, S. Xia, Rebamipide-loaded chitosan nanoparticles accelerate prostatic wound healing by inhibiting M1 macrophage-mediated inflammation via the NF-κB signaling pathway, Biomater. Sci. 8 (2020) 912–925.
[35] R. Eswaramoorthy, C.-C. Chang, S.-C. Wu, G.-J. Wang, J.-K. Chang, M.-L. Ho, Sustained release of PTH (1–34) from PLGA microspheres suppresses osteoarthritis progression in rats, Acta Biomater. 8(6) (2012) 2254–2262.
[36] R.E. Whitmire, D.S. Wilson, A. Singh, M.E. Levenston, N. Murthy, A.J. García, Self-assembling nanoparticles for intra-articular delivery of anti-inflammatory proteins, Biomaterials 33(30) (2012) 7665–7675.
[37] S. Pedroso-Santana, N. Fleitas-Salazar, Ionotropic gelation method in the synthesis of nanoparticles/microparticles for biomedical purposes, Polym. Int. 69(5) (2020) 443–447.
[38] D. Kong, E. Kusrini, L.D. Wilson, Binary pectin-chitosan composites for the uptake of lanthanum and yttrium species in aqueous media, Micromachines 12(5) (2021) 478.
[39] J. Mzoughi, T. Vandamme, V. Luchnikov, Biphasic drug release from rolled-up gelatin capsules with a cylindrical cavity, Pharmaceutics 13(12) (2021) 2040.
[40] J.J. Joseph, D. Sangeetha, T. Gomathi, Sunitinib loaded chitosan nanoparticles formulation and its evaluation, Int. J. Biol. Macromol. 82 (2016) 952–958.
[41] J. Emami, A. Pourmashhadi, H. Sadeghi, J. Varshosaz, H. Hamishehkar, Formulation and optimization of celecoxib-loaded PLGA nanoparticles by the Taguchi design and their *in vitro* cytotoxicity for lung cancer therapy, Pharmaceut. Dev. Technol. 20(7) (2015) 791–800.
[42] R. Seyedebrahimi, S. Razavi, J. Varshosaz, Controlled delivery of brain derived neurotrophic factor and gold-nanoparticles from chitosan/TPP nanoparticles for tissue engineering applications, J. Cluster Sci. 31 (2020) 99–108.
[43] B. Hu, C. Pan, Y. Sun, Z. Hou, H. Ye, B. Hu, X. Zeng, Optimization of fabrication parameters to produce chitosan−tripolyphosphate nanoparticles for delivery of tea catechins, J. Agric. Food Chem. 56(16) (2008) 7451–7458.
[44] H. Thakkar, R.K. Sharma, A.K. Mishra, K. Chuttani, R.S.R. Murthy, Efficacy of chitosan microspheres for controlled intra-articular delivery of celecoxib in inflamed joints, J. Pharm. Pharmacol. 56(9) (2004) 1091–1099.
[45] F.C. Iswanti, I. Nurulita, S. Djauzi, M. Sadikin, A.B. Witarto, T. Yamazaki, Preparation, characterization, and evaluation of chitosan-based nanoparticles as CpG ODN carriers, Biotechnol. Biotechnol. Equip. 33(1) (2019) 390–396.
[46] A. Jain, K. Thakur, G. Sharma, P. Kush, U.K. Jain, Fabrication, characterization and cytotoxicity studies of ionically cross-linked docetaxel loaded chitosan nanoparticles, Carbohydr. Polym. 137 (2016) 65–74.
[47] K. Liu, W. Chen, T. Yang, B. Wen, D. Ding, M. Keidar, J. Tang, W. Zhang, Paclitaxel and quercetin nanoparticles co-loaded in microspheres to prolong retention time for pulmonary drug delivery, Int. J. Nanomed. 12 (2017) 8239–8255.
[48] ISO 10993-4:2017, Biological Evaluation of Medical Devices—Part 4: Selection of Tests for Interactions with Blood, 2017.
[49] P. Venkatesan, N. Puvvada, R. Dash, B.N. Prashanth Kumar, D. Sarkar, B. Azab, A. Pathak, S.C. Kundu, P.B. Fisher, M. Mandal, The potential of celecoxib-loaded hydroxyapatite-chitosan nanocomposite for the treatment of colon cancer, Biomaterials 32(15) (2011) 3794–3806.
[50] R. Nadesh, P.R. Narayanan D., Sreerekha, S. Vadakumpully, U. Mony, M. Koyakkutty, S.V. Nair, D. Menon, Hematotoxicological analysis of surface-modified and -unmodified chitosan nanoparticles, J. Biomed. Mater. Res. 101 (2013) 2957–2966.
[51] M. Feldmann, F.M. Brennan, R.N. Maini, Role of cytokines in rheumatoid arthritis, Annu. Rev. Immunol. 14 (1996) 397–440.
[52] H. Sadeghpour, K. Roshan Nasrabad, M. Alipour Haghighi, A. Dehshahri, Preparation and characterization of celecoxib-conjugated polyethylenimine as a potential nanocarrier for gene delivery, Trends Pharm. Sci. 4(1) (2018) 17–28.